RESEARCH ARTICLE

Loss of chaperone-mediated autophagy does not alter age-related bone loss in male mice

James A. Hendrixson[1] | Alicen James[1] | Nisreen S. Akel[1] |
Dominique J. Laster[1] | Julie A. Crawford[2,3] | Stuart B. Berryhill[2,3] | Melda Onal[1]

[1]Department of Physiology and Cell Biology, University of Arkansas for Medical Sciences, Little Rock, Arkansas, USA

[2]Center for Musculoskeletal Disease Research (CMDR), University of Arkansas for Medical Sciences, Little Rock, Arkansas, USA

[3]Division of Endocrinology, University of Arkansas for Medical Sciences, Little Rock, Arkansas, USA

Correspondence
Melda Onal, Department of Physiology and Cell Biology, University of Arkansas for Medical Sciences, 4301 West Markham St., 505, Little Rock, AR 72205, USA.
Email: monal@uams.edu

Abstract

Chaperone-mediated autophagy (CMA) is a lysosome-dependent degradation pathway that eliminates proteins that are damaged, partially unfolded, or targeted for selective proteome remodeling. CMA contributes to several cellular processes, including stress response and proteostasis. Age-associated increase in cellular stressors and decrease in CMA contribute to pathologies associated with aging in various tissues. CMA contributes to bone homeostasis in young mice. An age-associated reduction in CMA was reported in osteoblast lineage cells; however, whether declining CMA contributes to skeletal aging is unknown. Herein we show that cellular stressors stimulate CMA in UAMS-32 osteoblastic cells. Moreover, the knockdown of an essential component of the CMA pathway, LAMP2A, sensitizes osteoblasts to cell death caused by DNA damage, ER stress, and oxidative stress. As elevations in these stressors are thought to contribute to age-related bone loss, we hypothesized that declining CMA contributes to the age-associated decline in bone formation by sensitizing osteoblast lineage cells to elevated stressors. To test this, we aged male CMA-deficient mice and controls up to 24 months of age and examined age-associated changes in bone mass and architecture. We showed that lack of CMA did not alter age-associated decline in bone mineral density as measured by dual x-ray absorptiometry (DXA). Moreover, microCT analysis performed at 24 months of age showed that vertebral cancellous bone volume, cortical thickness, and porosity of CMA-deficient and control mice were similar. Taken together, these results suggest that reduction of CMA does not contribute to age-related bone loss.

KEYWORDS
age-related bone loss, aging, cellular stress, chaperone-mediated autophagy, CMA, skeletal aging

Alicen James and James A. Hendrixson contributed equally to this work.

1 | INTRODUCTION

Autophagy is a recycling process via which cellular components, including individual proteins, protein aggregates, and organelles, are delivered to lysosomes for degradation. Autophagy is classified into three types based on the mechanisms by which cytoplasmic cargo is delivered to the lysosomes, namely macroautophagy, chaperone-mediated autophagy (CMA), and microautophagy.[1,2] In macroautophagy, cytoplasmic cargo is sequestered in double-membrane vesicles, termed autophagosomes, and delivered to lysosomes for degradation. In CMA, cargo is delivered to lysosomes via cytoplasmic chaperones, and in microautophagy, cytosolic cargo is entrapped directly by the invagination of the lysosomal membrane. Decreased macroautophagy is a bona fide hallmark of organismal aging that contributes to age-related pathologies in various tissues.[3] However, whether a decline in other types of autophagy contributes to aging at the organismal or tissue levels is not well established.

CMA is a selective form of autophagy that recycles individual proteins.[1,4] In CMA, proteins containing a KFERQ-like motif are recognized by cytoplasmic HSC70 and its co-chaperones and are delivered to lysosomes where they are unfolded and internalized by a translocation complex.[1,5,6] The CMA translocation complex is composed of lysosomal-associated membrane protein-2A (LAMP-2A) multimers.[4,5] Therefore, LAMP2A is an essential and rate-limiting component of CMA.[7] An age-associated decrease in LAMP2A levels reduces CMA in hepatocytes of old rats[8,9] and in late passage human fibroblasts.[8] This age-related decline in LAMP2A and CMA levels was also reported in several mouse cell types, such as hepatocytes,[10] hematopoietic stem cells (HSCs),[11] and fibroblasts.[9] In mouse hepatocytes and HSCs, genetic inhibition of CMA, via conditional deletion of *Lamp2a*, causes loss of protein homeostasis and accumulation of damaged proteins, and as a result accelerates age-associated cellular changes. In contrast, genetic or pharmaceutical restoration of CMA in hepatocytes or HSCs improves their protein homeostasis, decreases the age-associated accumulation of damaged proteins, and improves their cellular function.[11,12] In murine models of age-related diseases, such as atherosclerosis[13] and Alzheimer's disease,[14] CMA is reduced.[14] Inhibition of CMA exaggerates the disease pathologies observed in these murine disease models, whereas CMA stimulation alleviates the disease pathologies.[13,14] Together, these studies suggest that reduction in CMA contributes to aging pathologies in several tissues.

We previously showed that CMA contributes to bone homeostasis in young mice.[15] Specifically, we created a murine model in which two isoforms of *Lamp2*, namely *Lamp2A* and *Lamp2C*, were globally deleted from the mouse genome; we refer to this mouse model as L2ACgKO. Young adult L2ACgKO mice had lower vertebral cancellous bone mass than their littermate controls. Our ex vivo and in vitro studies suggested that this reduction in bone mass may be due to an inhibitory role of CMA for the production of osteoclasts (bone-resorbing cells) and a positive role of CMA in the formation or function of osteoblasts (bone-forming cells). In support of this, knockdown of *Lamp2a* in murine and human mesenchymal stem cells in culture decreased osteoblast formation.[16] In addition, immunohistochemistry for LAMP-2A expression showed that osteoblast lineage cells (progenitors and osteoblasts) from elderly people (>70 years) and aged C57BL/6 mice (16 months old) exhibit lower LAMP-2A protein levels compared to their young counterparts, suggesting an age-related decline in CMA in osteoblast lineage cells.[16] However, whether decline in CMA in osteoblast lineage cells contributes to the age-associated decline in bone formation is unknown. To test this idea, herein we examined age-related bone loss of L2ACgKO and control mice. Our results demonstrate that although CMA protects osteoblastic cells from age-associated cellular insults, lack of CMA does not alter age-related bone loss.

2 | MATERIALS AND METHODS

2.1 | Cell culture

Osteoblastic UAMS-32 cells were cultured in α-MEM containing 10% fetal bovine serum and 1% penicillin/streptomycin/glutamine. *Lamp2a* knockdown was performed as previously described.[15] Briefly, UAMS-32 cells were infected with lentivirus expressing *Lamp2a* shRNA (target sequence GAAGCACTTTGCTCCTTAAGA) or scrambled control (GeneCopoeia, vector psi-LVRU6GP). Cells stably expressing the shRNAs were selected via puromycin resistance. For mRNA or protein level assessment, cells were plated in six-well plates and exposed to cellular stressors for 6 h (for RNA) or 24 h (for protein). Starvation was performed by culturing cells in α-MEM without serum. For oxidative stress, cells were cultured with 10 or 500 μM H_2O_2 (Sigma, Cat. no. H1009). For DNA damage, cells were cultured with 100 μM etoposide (Fisher, Cat. no. AAJ63651MC). For the endoplasmic reticulum (ER) stress, cells were cultured with 0.5 μg/mL tunicamycin (Fisher, Cat. no. ICN15002810). RNA or protein was isolated for downstream analysis. For cell death measurements, 10,000 UAMS-32 shRNA control or shRNA *Lamp2a* cells were plated in each well of a 96-well plate. The next day, cells were treated with cellular stressors and cell death assays were performed 12–48 h after treatments as indicated in figure legends.

2.2 | Animals

Production of L2ACgKO mice was previously described.[15] Briefly, *Lamp2* exon 9A and *Lamp2* exon 9C were deleted from the mouse genome with CRISPR/Cas9 genome editing. We used DNA isolated from tail tips to genotype L2ACgKO mice and their littermates by PCR. The following primer sets were used for genotyping: one set whose product spans *Lamp2* exon 9A (forward 5′-GATGGCCCTACGGACTCTCT-3′ and reverse 5′-CCCCCAATGACTGCTTTTTA-3′) and a second set whose product lies within *Lamp2* exon 9A (forward 5′-AAAGCCAATCTGCATTTTAAGC-3′ and reverse 5′-TCTCAAGCGCCATCATACTG-3′). All mice were provided water and food ad libitum and were maintained on a 12-h light/dark cycle. All animal studies were carried out in accordance with the policies of, and with approval from, the Institutional Animal Care and Use Committee of the University of Arkansas for Medical Sciences. The studies described in this manuscript were performed and reported in accordance with ARRIVE guidelines. The sex, number, and age of the experimental mice are indicated in each figure legend.

2.3 | RNA isolation and gene expression analysis

Bones were dissected, cleaned of soft tissue, snap-frozen in liquid nitrogen, and stored at −80°C. For RNA isolation, lumbar vertebrae and tibia shafts were homogenized in Trizol Reagent (Life Technologies, Cat. no. 15596018). Next, RNA was isolated from homogenized bones with the RNAeasy Plus Mini Kit (Qiagen Cat. no. 74136) according to the manufacturer's instructions. RNA from cultured cells was isolated with Trizol Reagent (Life Technologies, Cat. no. 15596018) according to the manufacturer's instructions. RNA concentrations were determined with a Nanodrop instrument (Thermo Fisher Scientific). We used 1 μg of RNA to synthesize cDNA with a High-Capacity cDNA Reverse Transcription Kit (Applied Biosystems Cat. no. 4368814) and performed multiplex quantitative real-time PCR (qRT-PCR) with TaqMan Fast Advanced Master Mix (Applied Biosystems, Cat. no. 4444964), FAM-labeled TaqMan gene expression assays (Life Technologies), and VIC-labeled mouse *Actb* (β-actin) (Applied Biosystems, Cat. no. 4352341E) to quantify the relative mRNA levels. The following FAM-labeled assays were used in the gene expression analysis: *Rankl* (*Tnfsf11*, Mm00441906_m1), *Cathepsin K* (Mm00484039_m1), *Lamp2a = Lamp2-201* (Mm00495274_m1). The relative mRNA levels were calculated using the comparative cycle threshold (ΔCt) method.[17]

2.4 | Immunoblot analysis

Protein was extracted from the cultured cells using RIPA Buffer (Fisher Scientific, Cat. no. PI89901) with protease/phosphatase inhibitors (Cell Signaling Technologies, Cat. no. 5872S) according to the manufacturer's instructions. Proteins were then resolved in 4%−20% or 4%−15% Mini-PROTEAN TGX gels (BIORAD, Cat. no. 4561093 and Cat. no. 4561083, respectively) and transferred onto TransblotTurbo midi-size nitrocellulose membranes (0.2 μm pore size, BIORAD, Cat. no. 1704271). The membranes were blocked for 30 min with LI-COR Blocking Buffer-PBS (LI-COR, Cat. no. 4561083) and incubated overnight with primary antibodies and rocking at 4°C. The primary antibodies used were LAMP2A (Novus Biologicals, Cat. no. NBP267298, 1:1000 dilution) and β-actin (Millipore Sigma, Cat. no. A5316, 1:4000 dilution). After overnight incubation, membranes were washed three times with PBS and incubated for 45 min with appropriate secondary antibodies conjugated with IRDye 680 or IRDye 800 dyes (LI-COR, 1:2000 dilution). After washing with PBS, membranes were dried in the dark, scanned, and analyzed with an Odyssey IR imaging system (LI-COR) and Image Studio Software.

2.5 | Skeletal analysis

Bone mineral density (BMD) was measured in live mice by dual-energy x-ray absorptiometry (DXA) with a PIXImus Mouse Densitometer (GE Lunar Corp., Madison, WI) and the manufacturer's software as described previously.[18] The percentage of lean and fat mass was obtained from DXA analysis.

Fourth lumbar vertebrae (L4) and femurs were used for the microCT analysis. The femurs and vertebrae were dissected, cleaned of soft tissue, wrapped in saline-soaked gauze, and stored at −20°C. The microCT scans were performed on a model uCT40 (Scanco Biomedical) as previously described.[15,19] Briefly, medium-resolution scans were obtained (12 μm isotropic voxel size). A Gaussian filter (sigma = 0.8, support = 1) was used to reduce noise and a threshold of 220 was used for all scans. Nomenclature conforms to recommendations of the American Society for Bone and Mineral Research.[20] The midshaft cortical measurements were performed by drawing contours to measure the cortical thickness on the first 20 midshaft slices. Vertebral trabecular analysis was performed by drawing contours every 10 slices on the whole space between the two growth plates of the vertebrae. Calibration and quality control of the scanner were performed weekly or monthly as previously described.[21]

2.6 | Statistics

All values are reported as mean ± standard deviation (SD). Differences between the two genotypes (WT vs. L2ACgKO) were evaluated using GraphPad Prism 7.05 software (GraphPad Software, Inc, La Jolla, CA, USA). The specific statistical tests and number of replicates performed are indicated in figure legends.

3 | RESULTS

3.1 | CMA protects osteoblastic cells from cellular stressors that are thought to contribute to pathologies associated with aging

Increased cellular stressors and reduced stress-response mechanisms are thought to contribute to pathologies associated with aging in various tissues including bone.[22,23] Specifically, the age-associated elevation of oxidative, genotoxic, and ER stress has been proposed to contribute to age-related bone loss.[24–27]

To test whether elevated CMA protects osteoblastic cells from cellular stressors, we first examined whether CMA in osteoblasts increases in response to cellular stressors. We exposed an osteoblastic cell line (UAMS-32 cells) to prolonged serum starvation, oxidative stress induced by H_2O_2, genotoxic stress induced by etoposide, or ER stress induced by tunicamycin. In other cell types, LAMP2A levels and—as a consequence—CMA levels increase in response to these cellular stressors.[28,29] Consistent with this finding, LAMP2A protein levels increased in cultured osteoblastic cells exposed to starvation, oxidative, genotoxic, and ER stress (Figure 1A). We next showed that oxidative and genotoxic stress, but not ER stress, increased LAMP2A levels by elevating transcription of *Lamp2a* (Figure 1B). This is consistent with previous observations showing that ER stress does not induce CMA via transcriptional upregulation of *Lamp2a* levels. Instead, ER stress induces post-translational modification of LAMP2A, which activates LAMP2A and drives LAMP2A accumulation on the lysosomal membrane, thus inducing CMA.[30] Together these results suggests that CMA increases in response to cellular stressors also in osteoblastic cells.

Next, we sought to address if the stress-induced increase in CMA is protective from cell death induced by these cellular stressors. For this purpose, we knocked down LAMP2A in UAMS-32 cells (Figure 1B) and compared stress-induced cell death of CMA-deficient and control cells. Similar to what has been observed in other cell types,[7] CMA-deficient cells were more vulnerable to cell death induced by oxidative stress, genotoxic and ER stress, than control cells (Figure 1C). These results suggest that CMA also protects osteoblasts from cellular stressors.

3.2 | CMA deficiency increases RANKL expression induced by ER stress

DNA damage and ER stress stimulate the production of the proresorptive cytokine receptor activator of NF-κB ligand (RANKL).[31–33] Stimulation of RANKL by these cellular stressors is thought to contribute to the increase in bone resorption and thereby contribute to bone loss in pathological conditions associated with elevated DNA damage[33] and ER stress.[31] We have previously shown that CMA deficiency causes an increase in *Rankl* (*Tnfsf11*) mRNA levels in vitro and in vivo[15]; however, whether CMA influences DNA-damage- or ER stress- induced elevation of RANKL is unknown. To test this, we exposed UAMS-32 cells to genotoxic stress induced by etoposide or ER stress induced by tunicamycin. As previously shown, both etoposide and tunicamycin increased *Rankl* mRNA levels in control cells (Figure 2). CMA deficiency exaggerated the increase in *Rankl* mRNA levels caused by ER stress, but did not alter the DNA-damage-induction of *Rankl* (Figure 2). These results suggest that CMA deficiency, via increasing RANKL production, may exaggerate bone resorption induced by ER stress.

3.3 | Age-associated bone loss is not altered by CMA deficiency

Our in vitro studies suggest that CMA deficiency makes osteoblast lineage cells more vulnerable to various cellular stressors that are known to increase with age, and exaggerates stimulation of RANKL induced by ER stress. Based on these findings, and the previously reported age-associated reduction in LAMP2A levels in osteoblast progenitors of mice and humans,[16] we hypothesized that a reduction in CMA contributes to age-associated bone loss. If this hypothesis is correct, CMA deficiency should accelerate and accentuate age-related changes in bone, as it does in hepatocytes or HSCs.[10,11]

To test whether CMA deficiency accelerated age-related bone loss, we aged two cohorts of male wild-type and CMA-deficient mice up to 24 months of age and measured their BMD at different time points. We measured BMD of one cohort of mice at 9, 12, and 14 months of age (cohort 1, Figure 3A–C), and another cohort of mice at 9 and 17 months of age (cohort 2, Figure 3D–F). In both cohorts of mice, aging reduced BMD at all sites measured independent of the genotype of mice (Figure 3), suggesting that CMA deficiency does not accelerate age-related bone loss.
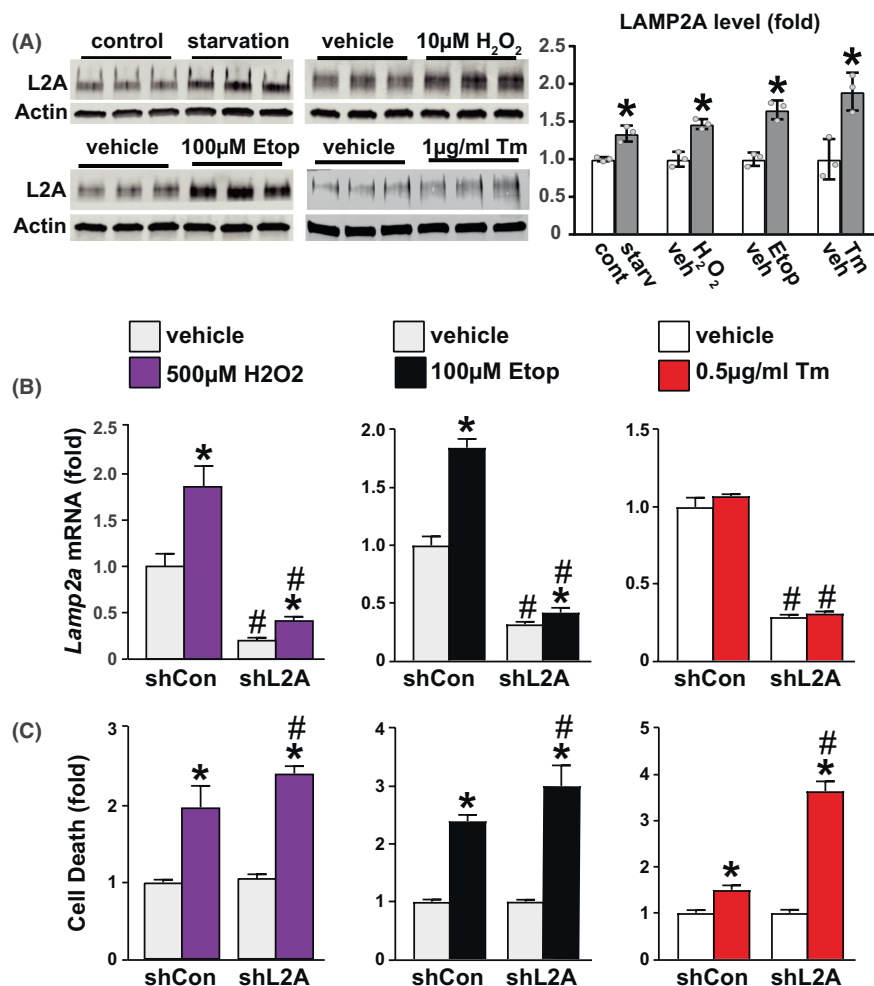
FIGURE 1 Osteoblasts use CMA as a stress-response mechanism. (A) Immunoblot of LAMP2A (L2A) levels in osteoblastic UAMS-32 cells in response to 24 h of starvation, oxidative stress induced by hydrogen peroxide (H_2O_2), genotoxic stress induced by etoposide (Etop), and ER stress induced by tunicamycin (Tm). (B, C) UAMS-32 cells stably expressing scrambled shRNA (shCon) or shRNA targeting *Lamp2a* (shL2A) were treated with vehicle (DMSO), 0.5 μg/mL Tm, 100 μM Etop, and 500 μM H_2O_2. (B) Quantitative real-time PCR (qRT-PCR) was used to measure *Lamp2a* mRNA levels 6 h after treatments ($n=6$ wells/group). (C) Tm-induced apoptosis was measured 12 h after treatment by caspase 3/7 activation ($n=6$ wells/group). Etop- and H_2O_2-induced cell death was measured by CellTox Green Assay 48 h and 24 h after treatment, respectively. ($n=3$ wells/group). Bars indicate mean ± standard deviation (SD). * $p<0.05$ effect of treatment; # $p<0.05$ effect of genotype by two-way ANOVA.

Next, we tested whether CMA deficiency accentuates skeletal aging with advanced age, by aging both cohorts of mice and comparing the male wild-type and CMA-deficient mice at 24 months of age. Of note, ER stress, DNA damage, and oxidative stress have all previously been shown to be elevated in osteoblastic lineage cells at 24 months of age.[24,26,32] Mice deficient in CMA had a modest increase in *Rankl* mRNA levels in the cortical bones of 24-month-old mice (Figure 4A); however, this change in RANKL levels was not sufficient to alter bone turnover as the thickness and porosity of the cortical bone were similar in both wild-type and L2ACgKO mice (Figure 4B). As measured by gene expression of osteoclast and osteoblast markers (e.g., *CtsK, Acp5, Col1a1, Bglap*), CMA deficiency did not alter bone

turnover in the spine (Figure 4C). Accordingly, vertebral cancellous bone mass and architecture of wild-type and CMA-deficient mice were similar at 24 months of age (Figure 4D). Similarly, at 24 months of age, bone volume, and architecture of female wild-type and CMA-deficient mice were also comparable (Figure 5). These findings indicate that CMA deficiency did not accentuate age-related bone loss.

3.4 | CMA deficiency does not alter age-related changes in body composition

Previous studies found that lack of *Lamp2a*, and thereby CMA, either specifically in the liver or globally in all
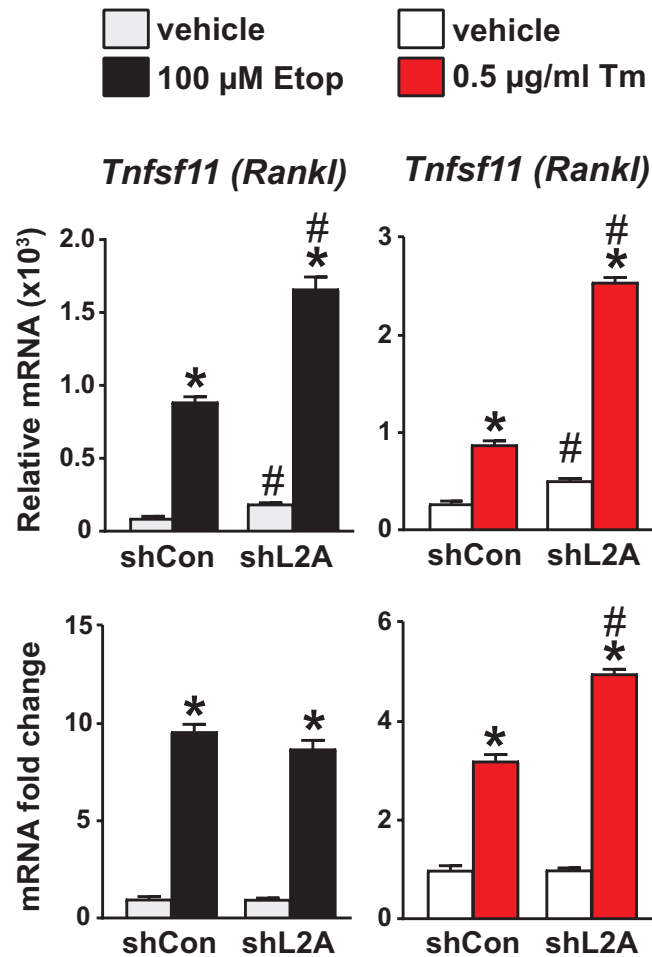
FIGURE 2 CMA deficiency exaggerates RANKL expression induced by ER stress. Osteoblastic UAMS-32 cells stably expressing scrambled shRNA (shCon) or shRNA targeting *Lamp2a* (shL2A) were treated for 6 h with vehicle (Vehicle, DMSO), 0.5 μg/mL tunicamycin (Tm) or 100 μM etoposide (Etop). qRT-PCR was used to measure *Rankl (Tnfsf11)* mRNA levels. *Rankl* mRNA levels were normalized to β-actin (top panel). Fold change was calculated by normalizing to vehicle treatment of each genotype (bottom panel). ($n = 6$ wells/group). Bars indicate mean ± SD. * $p < 0.05$ effect of treatment; # $p < 0.05$ effect of genotype by two-way ANOVA.

tissues, alters metabolism and body composition in young mice.[13,34] Specifically, these studies showed that young CMA-deficient mice are more susceptible to starvation-induced weight loss[34] and high-fat diet-induced weight gain.[13] Both were reported to be mostly due to effects on fat mass content. To test whether CMA deficiency alters age-associated changes in body composition, we compared body weight, fat mass, and lean mass of two cohorts of male mice that were fed a regular chow diet. Body weight of both wild-type and L2ACgKO male mice increased with age (Figure 6A,D). This increase in body weight in L2ACgKO mice was associated with a decrease in lean mass (Figure 6B,E) and an increase in fat mass (Figure 6C,D). Similar trends were observed in wild-type mice (Figure 6). Overall, wild-type and CMA-deficient mice showed no significant differences in body weight or body composition up to 17 months of age (Figure 6). These findings indicate that CMA deficiency does not alter age-related changes in body weight or body composition of male mice.

4 | DISCUSSION

We previously showed that CMA contributes to the accrual and maintenance of vertebral cancellous bone in young adult mice[15] and that it may do so by contributing to osteoblast differentiation.[15,16,35] However, whether CMA plays additional roles in osteoblast lineage cells was unknown. Herein, we used an osteoblastic cell line and showed that like other cell types, osteoblastic cells use CMA as a stress-response mechanism. Age-related elevation of cellular stressors is thought to contribute to age-related bone loss,[23,26,36] and an age-associated decline in CMA was observed in murine and human osteoblast lineage cells.[16] However, whether the decline of this stress-response pathway functionally contributes to age-associated bone loss was unknown. To address this, we aged mice with global CMA deficiency up to 24 months of age. We found that lack of CMA did not alter age-related bone loss, suggesting that the age-associated decline in CMA does not functionally contribute to skeletal aging.
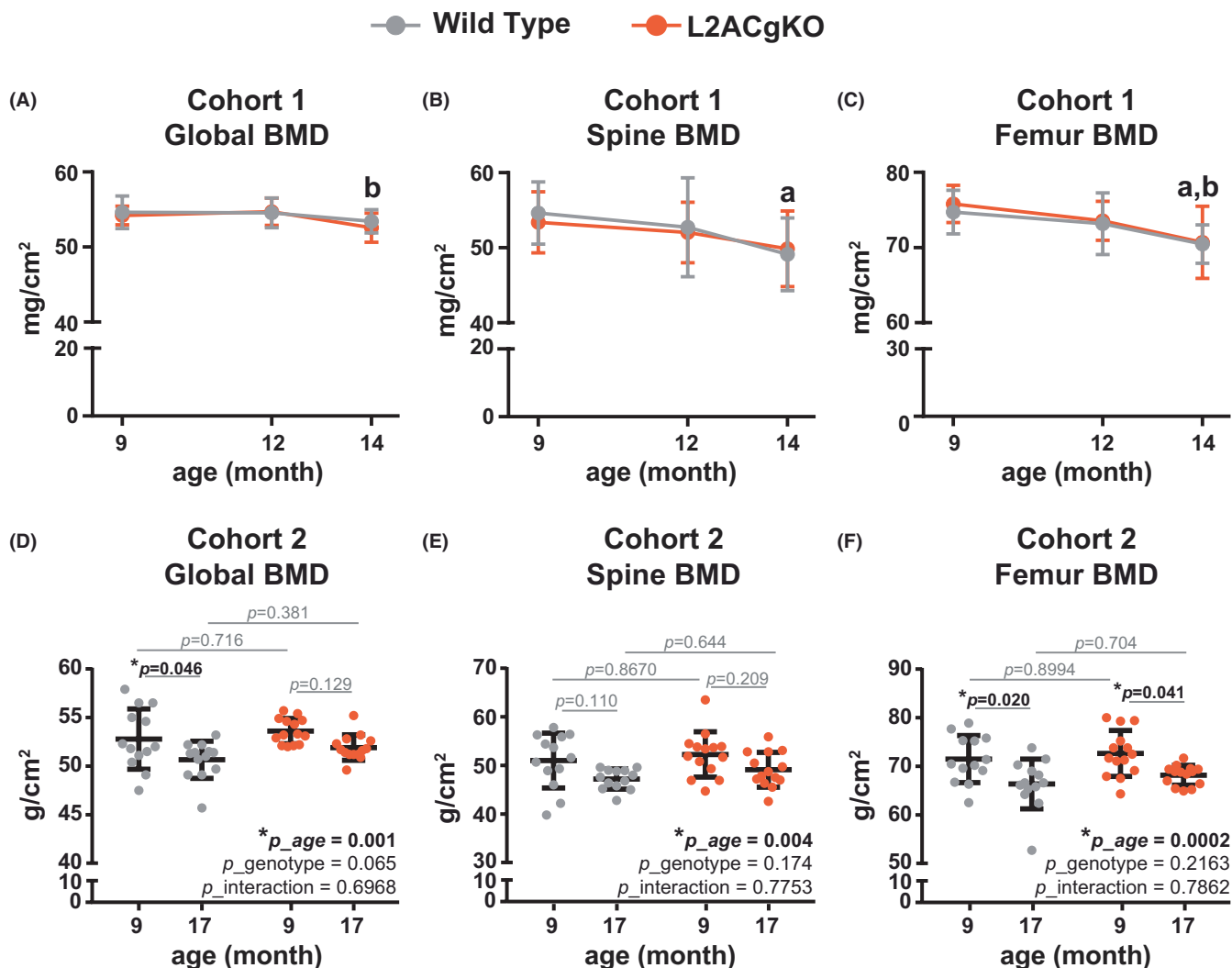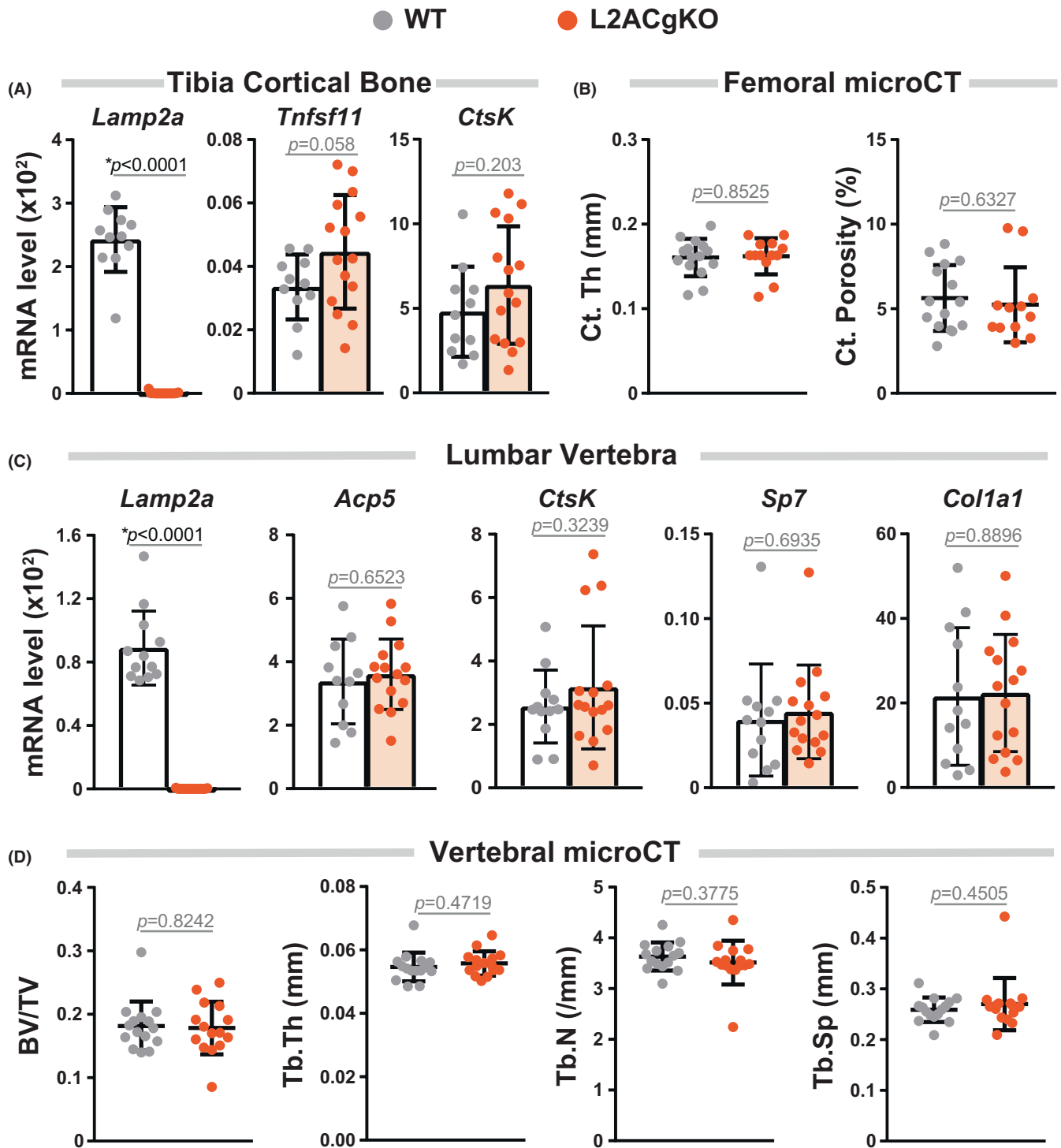
FIGURE 3 CMA deficiency does not accelerate age-related bone loss. Total body, vertebral, and femoral bone mineral density (BMD) of male L2ACgKO and their wild-type (WT) littermates were measured at 9, 12, and 14 months of age (cohort 1, A–C) or 9 and 17 months of age (cohort 2, D–F) with DXA Piximus. Bars indicate mean ± SD. (A–C), Cohort 1 is $n = 7$–10 mice/group. a, $p < 0.05$ comparing 12-month or 14-month L2ACgKO to 9-month L2ACgKO with Student's t-test. b, $p < 0.05$ comparing 12-month or 14-month WT to 9-month WT with Student's t-test. c, $p < 0.05$ comparing WT to L2ACgKO of the same age with Student's t-test. (D, E), Cohort 2 is $n = 13$–14 mice/group. * $p < 0.05$ using two-way ANOVA. The individual p-value of each comparison is indicated on the graphs.

Studies by us and others suggest that age-associated dysfunction in different types of autophagy contributes at different levels to organismal and tissue aging. For instance, in murine models, global loss of macroautophagy decreases lifespan,[37,38] whereas, restoration of macroautophagy increases lifespan and healthspan,[39–41] thus establishing disabled macroautophagy as a bona fide hallmark of organismal aging.[3] In contrast, we and others[14] did not observe drastic changes in mortality or lifespan in CMA-deficient mice, suggesting that declining CMA is not a significant contributor to organismal aging. Rather, declining CMA seems to contribute to age-related pathologies in a tissue-specific manner. Specifically, although declining CMA in hepatocytes, HSC, macrophages, and neurons contributes to age-related pathologies, declining

CMA in osteoblast lineage cells does not contribute to skeletal aging.

Age-associated bone loss occurs through different cellular mechanisms in the cancellous and cortical compartments. In the cancellous compartment, the decrease in trabecular bone volume is associated with a low rate of bone remodeling.[24] Whereas, age-associated thinning and elevated porosity of the cortical bone is associated with increased bone remodeling.[19] As deletion of *Lamp2a* is global in our model, L2ACgKO mice also lack CMA in osteoclasts. While we did not specifically examine the role of CMA in osteoclasts; osteoclast marker gene expression, cortical thickness, and cortical porosity were unaltered by CMA deficiency in old mice (Figure 4), suggesting that loss of CMA does not alter age-associated changes in osteoclasts or bone resorption.

FIGURE 4 CMA deficiency does not exaggerate age-related bone loss. Male Lamp2AC global knockout (L2ACgKO) mice and their wild-type (WT) littermates were aged up to 24 months of age. At this age, animals were sacrificed and microCT (μCT) and gene expression analyses were performed. (A) mRNA levels of *Lamp2a*, *Rankl* (*Tnfsf11*), and *CstK* in tibia shafts were measured by qRT-PCR and normalized to β-actin levels. (B, C) μCT analysis was performed on femurs and lumbar vertebrae from four 24-month-old male L2ACgKO mice and their littermate controls. (B) Cortical thickness (Ct.Th) was measured at the femoral midshaft, and cortical porosity was measured at the femoral metaphysis as previously described.[49] (C) Cancellous bone volume over tissue volume (BV/TV), trabecular thickness (Tb.Th), trabecular number (Tb.N), and trabecular separation (Tb.Sp) were measured in lumbar vertebrae 4. (D) RNA levels of *Lamp2a*, *Acp5* (*Trap*), *CstK*, *Sp7* (*Osx1), and Col1a1* levels were measured in lumbar vertebrae 5 by qRT-PCR and normalized to β-actin levels. (*n* = 11–15 mice/group). Bars indicate mean ± SD. * *p* < 0.05 by Student's *t*-test. The individual *p*-value of each comparison is indicated on the graphs.
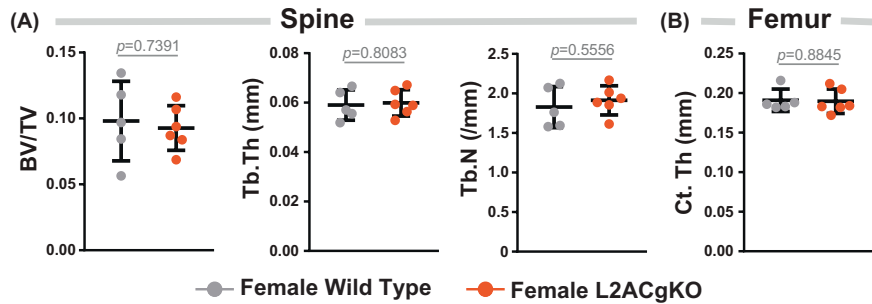
FIGURE 5 CMA deficiency does not alter the cancellous or cortical bone of old female mice. Female Lamp2AC global knockout (L2ACgKO) mice and their wild-type (WT) littermates were aged up to 24 months of age. At this age, animals were sacrificed and microCT (μCT) analysis was performed. (A) Cancellous bone volume over tissue volume (BV/TV), trabecular thickness (Tb.Th), and trabecular number (Tb.N) were measured in lumbar vertebrae 4. (B) Cortical thickness (Ct.Th) was measured at the femoral midshaft. ($n = 5$–6 mice/group). Bars indicate mean $\pm$ SD. * $p < 0.05$ by Student's t-test.
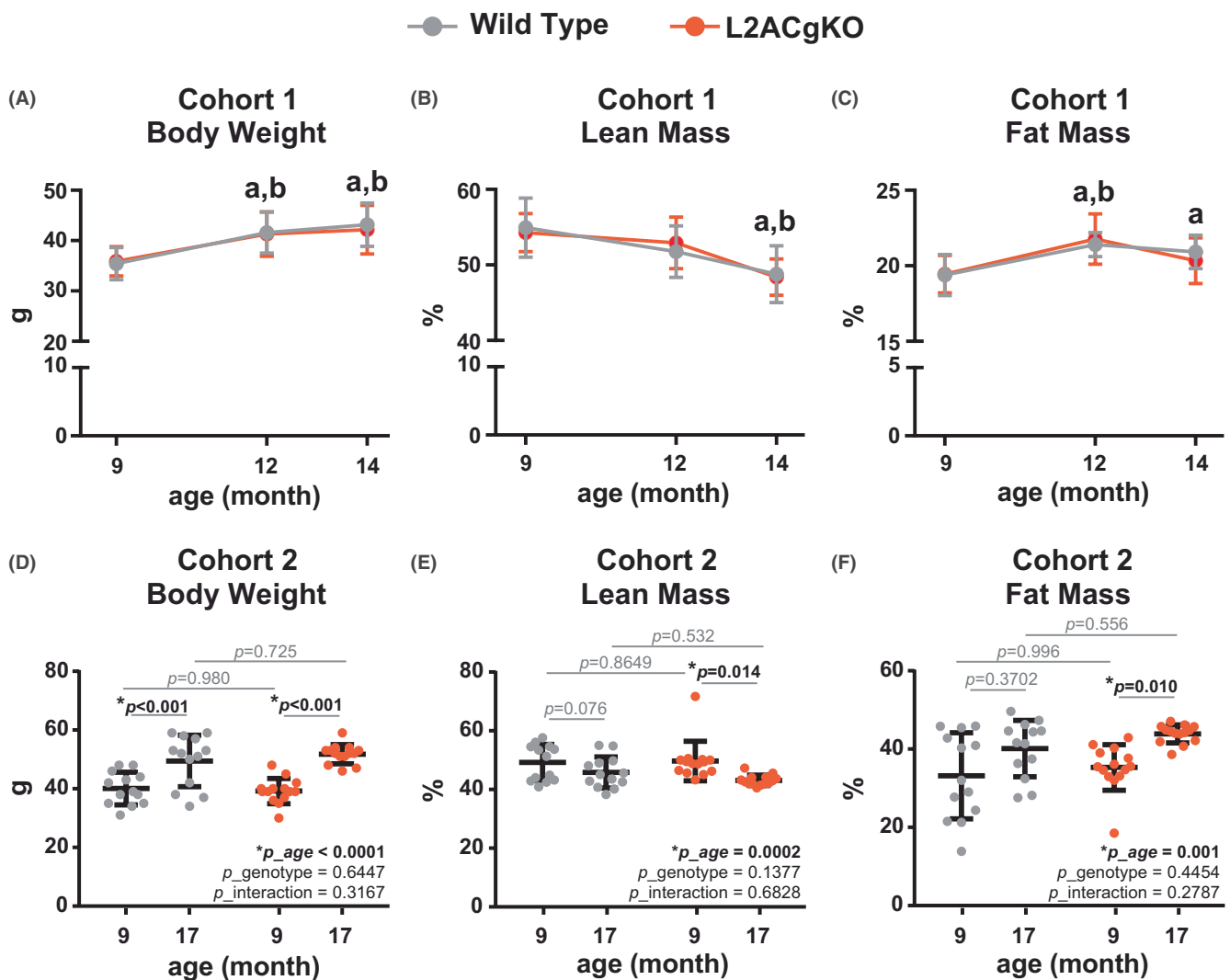
FIGURE 6 CMA deficiency does not alter age-associated changes in body mass or composition. Body weight in grams (g) (A), lean mass normalized to body mass (%) (B), and fat mass normalized to body mass (%) (C) were measured with DXA Piximus at 9, 12, and 14 months of age (cohort 1, A–C) or 9 and 17 months of age (cohort 2, D–F). Bars indicate mean $\pm$ SD. (A–C), Cohort 1 is $n = 7$–10 mice/group. a, $p < 0.05$ comparing 12-month or 14-month L2ACgKO to 9-month L2ACgKO with Student's t-test. b, $p < 0.05$ comparing 12-month or 14-month WT to 9-month WT with Student's t-test. c, $p < 0.05$ comparing WT to L2ACgKO of the same age with Student's t-test. (D, E) Cohort 2 is $n = 13$–14 mice/group. * $p < 0.05$ using two-way ANOVA. The individual p-value of each comparison is indicated on the graphs.

Prior studies have noted the influence of sex on skeletal aging.[19] One limitation of our study is that majority of our analysis is performed in male mice because we did not have a sufficient number of female mice to obtain strong statistical power. Even so, our preliminary analysis with a limited number of female mice did not reveal any drastic differences in cancellous bone volume or cortical thickness of aged CMA-deficient and control mice (Figure 5). However, it was previously noted that female C57Bl/6 mice are more prone to developing age-associated increases in cortical porosity than male mice.[19] Based on this, although we were able to detect the similar levels of cortical porosity in both CMA-deficient and control male mice in our studies, we cannot exclude the possibility that female mice may exhibit increased intracortical remodeling, which may be exaggerated by CMA deficiency.

In culture, CMA deficiency made osteoblastic cells more vulnerable to age-associated cellular stressors. However, in vivo CMA deficiency did not accelerate or accentuate age-associated bone loss. There are a few potential explanations for this. One possibility is that cellular stress levels in old bones in vivo are not as high as the chemical induction of these stressors in vitro. In support of this, while Chalil et al. noted elevated ER stress markers in osteocyte-enriched ex vivo cultures obtained from old versus young mice, tunicamycin treatment of the same cultures resulted in elevation of these markers to a greater extent.[26] Therefore, further studies are necessary to address if CMA is more important in pathological conditions with chronic induction of ER stress, such as that which occurs due to misfolding of collagen in osteogenesis imperfecta.[42,43] CMA may also be important for other stress-associated skeletal pathologies. For instance, ER stress and oxidative stress are thought to contribute to glucocorticoid-induced apoptosis of osteoblast lineage cells and thereby contribute to glucocorticoid-induced bone loss.[44–47] In neurons, glucocorticoids suppress CMA.[48] However, whether glucocorticoids suppress CMA in the osteoblast lineage and if so, whether this suppression contributes to glucocorticoid-induced osteoblast or osteocyte apoptosis is unknown.

Herein we show that osteoblastic cells use CMA as a stress-response mechanism; however, decreased CMA activity in the osteoblast lineage does not contribute to age-related bone loss. Moreover, we show that CMA does not play a role in age-associated changes in body weight or composition. Overall, our studies suggest that the functional contribution of declining CMA to age-associated pathologies is cell-type- and context-dependent.

AUTHOR CONTRIBUTIONS

A.J., M.O., and N.A. performed cell culture work. N.A. performed DXA BMD measurements. D.J.L., J.A.C.,and M.O. euthanized the mice and collected tissue. A.J. and J.A.H. performed microCT analysis. S.B.H. performed femoral porosity analysis. J.A.H. performed gene expression analysis. A.J. and M.O. performed the statistical analysis and prepared the manuscript.

ACKNOWLEDGMENTS

FUNDING INFORMATION

DISCLOSURES

The authors state that they have no conflicts of interest.

DATA AVAILABILITY STATEMENT

The datasets generated during the current study are available from the corresponding author on reasonable request.

ORCID

James A. Hendrixson https://orcid.org/0009-0004-5175-2357
Alicen James https://orcid.org/0009-0006-4750-4419
Nisreen S. Akel https://orcid.org/0009-0007-7326-7020
Dominique J. Laster https://orcid.org/0009-0008-1285-2020
Julie A. Crawford https://orcid.org/0000-0002-8167-8627
Stuart B. Berryhill https://orcid.org/0009-0003-5119-1062
Melda Onal https://orcid.org/0000-0002-5804-495X

REFERENCES

1. Kaushik S, Cuervo AM. The coming of age of chaperone-mediated autophagy. *Nat Rev Mol Cell Biol*. 2018;19:365-381.
2. Feng Y, He D, Yao Z, Klionsky DJ. The machinery of macroautophagy. *Cell Res*. 2014;24:24-41.
3. Lopez-Otin C, Blasco MA, Partridge L, Serrano M, Kroemer G. Hallmarks of aging: an expanding universe. *Cell*. 2023;186:243-278.
4. Cuervo AM, Dice JF. A receptor for the selective uptake and degradation of proteins by lysosomes. *Science*. 1996;273:501-503.
5. Cuervo AM, Dice JF. Unique properties of lamp2a compared to other lamp2 isoforms. *J Cell Sci*. 2000;113(24):4441-4450.
6. Bandyopadhyay U, Sridhar S, Kaushik S, Kiffin R, Cuervo AM. Identification of regulators of chaperone-mediated autophagy. *Mol Cell*. 2010;39:535-547.

7. Massey AC, Kaushik S, Sovak G, Kiffin R, Cuervo AM. Consequences of the selective blockage of chaperone-mediated autophagy. *Proc Natl Acad Sci U S A*. 2006;103:5805-5810.

8. Cuervo AM, Dice JF. Age-related decline in chaperone-mediated autophagy. *J Biol Chem*. 2000;275:31505-31513.

9. Kiffin R, Kaushik S, Zeng M, et al. Altered dynamics of the lysosomal receptor for chaperone-mediated autophagy with age. *J Cell Sci*. 2007;120:782-791.

10. Schneider JL, Villarroya J, Diaz-Carretero A, et al. Loss of hepatic chaperone-mediated autophagy accelerates proteostasis failure in aging. *Aging Cell*. 2015;14:249-264.

11. Dong S, Wang Q, Kao YR, et al. Chaperone-mediated autophagy sustains haematopoietic stem-cell function. *Nature*. 2021;591:117-123.

12. Zhang C, Cuervo AM. Restoration of chaperone-mediated autophagy in aging liver improves cellular maintenance and hepatic function. *Nat Med*. 2008;14:959-965.

13. Madrigal-Matute J, de Bruijn J, van Kuijk K, et al. Protective role of chaperone-mediated autophagy against atherosclerosis. *Proc Natl Acad Sci U S A*. 2022;119:e2121133119.

14. Bourdenx M, Martín-Segura A, Scrivo A, et al. Chaperone-mediated autophagy prevents collapse of the neuronal metastable proteome. *Cell*. 2021;184:2696-2714 e2625.

15. Akel N, MacLeod RS, Berryhill SB, et al. Loss of chaperone-mediated autophagy is associated with low vertebral cancellous bone mass. *Sci Rep*. 2022;12:3134.

16. Gong Y, Li Z, Zou S, et al. Vangl2 limits chaperone-mediated autophagy to balance osteogenic differentiation in mesenchymal stem cells. *Dev Cell*. 2021;56:2103-2120.e9.

17. Livak KJ, Schmittgen TD. Analysis of relative gene expression data using real-time quantitative PCR and the 2(-Delta Delta C(T)) method. *Methods*. 2001;25:402-408.

18. Onal M, Bishop KA, St John HC, et al. A DNA segment spanning the mouse Tnfsf11 transcription unit and its upstream regulatory domain rescues the pleiotropic biologic phenotype of the RANKL null mouse. *J Bone Miner Res*. 2015;30:855-868.

19. Piemontese M, Almeida M, Robling AG, et al. Old age causes de novo intracortical bone remodeling and porosity in mice. *JCI Insight*. 2017;2:e93771.

20. Bouxsein ML, Boyd SK, Christiansen BA, Guldberg RE, Jepsen KJ, Müller R. Guidelines for assessment of bone microstructure in rodents using micro-computed tomography. *J Bone Miner Res*. 2010;25:1468-1486.

21. MacLeod RS, Cawley KM, Gubrij I, Nookaew I, Onal M, O'Brien CA. Effective CRISPR interference of an endogenous gene via a single transgene in mice. *Sci Rep*. 2019;9:17312.

22. Kourtis N, Tavernarakis N. Cellular stress response pathways and ageing: intricate molecular relationships. *EMBO J*. 2011;30:2520-2531.

23. Almeida M, O'Brien CA. Basic biology of skeletal aging: role of stress response pathways. *J Gerontol A Biol Sci Med Sci*. 2013;68:1197-1208.

24. Almeida M, Han L, Martin-Millan M, et al. Skeletal involution by age-associated oxidative stress and its acceleration by loss of sex steroids. *J Biol Chem*. 2007;282:27285-27297.

25. Almeida M. Aging mechanisms in bone. *Bonekey Rep*. 2012;1:102.

26. Chalil S, Jaspers RT, Manders RJ, Klein-Nulend J, Bakker AD, Deldicque L. Increased endoplasmic reticulum stress in mouse osteocytes with aging alters Cox-2 response to mechanical stimuli. *Calcif Tissue Int*. 2015;96:123-128.

27. Suzuki R, Fujiwara Y, Saito M, et al. Intracellular accumulation of advanced glycation end products induces osteoblast apoptosis via endoplasmic reticulum stress. *J Bone Miner Res*. 2020;35:1992-2003.

28. Kiffin R, Christian C, Knecht E, Cuervo AM. Activation of chaperone-mediated autophagy during oxidative stress. *Mol Biol Cell*. 2004;15:4829-4840.

29. Park C, Suh Y, Cuervo AM. Regulated degradation of Chk1 by chaperone-mediated autophagy in response to DNA damage. *Nat Commun*. 2015;6:6823.

30. Li W, Zhu J, Dou J, et al. Phosphorylation of LAMP2A by p38 MAPK couples ER stress to chaperone-mediated autophagy. *Nat Commun*. 2017;8:1763.

31. Iyer S, Melendez-Suchi C, Han L, Baldini G, Almeida M, Jilka RL. Elevation of the unfolded protein response increases RANKL expression. *FASEB Bioadv*. 2020;2:207-218.

32. Kim HN, Chang J, Shao L, et al. DNA damage and senescence in osteoprogenitors expressing Osx1 may cause their decrease with age. *Aging Cell*. 2017;16:693-703.

33. Kim HN, Xiong J, MacLeod RS, et al. Osteocyte RANKL is required for cortical bone loss with age and is induced by senescence. *JCI Insight*. 2020;5:e138815.

34. Schneider JL, Suh Y, Cuervo AM. Deficient chaperone-mediated autophagy in liver leads to metabolic dysregulation. *Cell Metab*. 2014;20:417-432.

35. Wang Y, Hang K, Ying L, et al. LAMP2A regulates the balance of mesenchymal stem cell adipo-osteogenesis via the Wnt/beta-catenin/GSK3beta signaling pathway. *J Mol Med (Berl)*. 2023;101:783-799.

36. Chen Q, Liu K, Robinson AR, et al. DNA damage drives accelerated bone aging via an NF-κB-dependent mechanism. *J Bone Miner Res*. 2013;28:1214-1228.

37. Cassidy LD, Young ARJ, Young CNJ, et al. Temporal inhibition of autophagy reveals segmental reversal of ageing with increased cancer risk. *Nat Commun*. 2020;11:307.

38. Karsli-Uzunbas G, Guo JY, Price S, et al. Autophagy is required for glucose homeostasis and lung tumor maintenance. *Cancer Discov*. 2014;4:914-927.

39. Wang C, Haas M, Yeo SK, et al. Enhanced autophagy in Becn1(F121A/F121A) knockin mice counteracts aging-related neural stem cell exhaustion and dysfunction. *Autophagy*. 2022;18:409-422.

40. Fernandez AF, Sebti S, Wei Y, et al. Disruption of the beclin 1-BCL2 autophagy regulatory complex promotes longevity in mice. *Nature*. 2018;558:136-140.

41. Sebti S, Zou Z, Shiloh MU. BECN1(F121A) mutation increases autophagic flux in aged mice and improves aging phenotypes in an organ-dependent manner. *Autophagy*. 2023;19:957-965.

42. Mirigian LS, Makareeva E, Mertz EL, et al. Osteoblast malfunction caused by cell stress response to procollagen misfolding in α2(I)-G610C mouse model of osteogenesis imperfecta. *J Bone Miner Res*. 2016;31:1608-1616.

43. Besio R, Garibaldi N, Leoni L, et al. Cellular stress due to impairment of collagen prolyl hydroxylation complex is rescued by the chaperone 4-phenylbutyrate. *Dis Model Mech*. 2019;12:dmm038521.

44. O'Brien CA, Jia D, Plotkin LI, et al. Glucocorticoids act directly on osteoblasts and osteocytes to induce their apoptosis and reduce bone formation and strength. *Endocrinology.* 2004;145:1835-1841.

45. Hurson CJ, Butler JS, Keating DT, et al. Gene expression analysis in human osteoblasts exposed to dexamethasone identifies altered developmental pathways as putative drivers of osteoporosis. *BMC Musculoskelet Disord.* 2007;8:12.

46. Manolagas SC. From estrogen-centric to aging and oxidative stress: a revised perspective of the pathogenesis of osteoporosis. *Endocr Rev.* 2010;31:266-300.

47. Sato AY, Tu X, McAndrews KA, Plotkin LI, Bellido T. Prevention of glucocorticoid induced-apoptosis of osteoblasts and osteocytes by protecting against endoplasmic reticulum (ER) stress in vitro and in vivo in female mice. *Bone.* 2015;73:60-68.

48. Sato M, Ueda E, Konno A, et al. Glucocorticoids negatively regulates chaperone mediated autophagy and microautophagy. *Biochem Biophys Res Commun.* 2020;528:199-205.

49. Zebaze RM, Ghasem-Zadeh A, Bohte A, et al. Intracortical remodelling and porosity in the distal radius and post-mortem femurs of women: a cross-sectional study. *Lancet.* 2010;375:1729-1736.